Physical Sciences and Technology. Vol. 7 (No. 3-4), 2020: 36-42

IRSTI 29.05.03 https://doi.org/10.26577/phst.2020.v7.i2.06

Current and capacitance hysteresis in porous semiconductor nanofilms

Z.Zh. Zhanabaev, D.A. Turlykozhayeva*, S.B. Ikramova, A.O. Tileu, A.A. Maksutova, B.A. Khaniyev, A.K. Khaniyeva

Department of Solid State Physics and Nonlinear Physics, Al-Farabi Kazakh National University, 71 al-Farabi Avenue, 050040, Almaty, Kazakhstan
e-mail: Dana.Turlykozhayeva@kaznu.kz

At present, the study of complex electro-physical characteristics of semiconductor nanofilaments and nanofilms is of interest: the presence of non-monotonic oscillating characteristics with memory, areas of negative differential resistance. The aim of this work is to experimentally study both the volt-ampere and volt-farad characteristics of semiconductor nanoporous structures. The studied samples of porous silicon with the p-n structure were obtained by electrochemical etching. Single-crystal silicon with a p – n+ junction was used as the initial substrate. The NI EL VIS II+ educational platform and the Agilent E4980A instrument were used to study the electrophysical characteristics. To measure the dependence of current on voltage, as well as capacitance on voltage, Inga contacts with a thickness of 370 nm each were applied to nanoporous films. Thus, in this work, the phenomena of current switching, hysteresis behavior of current, and capacitance of porous silicon nanofilms are experimentally studied. It was found that these effects are amplified by a factor of 3-4 when the films are irradiated with an infrared laser. The results of this work can be used in the field of nanotechnology to improve memory and sensory elements. The established experimental facts can serve as a basis for constructing physical theories.

Key words: Por-Si, Current-voltage characteristic, Volt-farad characteristic, Hysteresis
PACS numbers: 61.46.-w, 61.46.Km, 62.63.Hj, 73.63.-b.

1 Introduction

Porous silicon (por-Si) obtained by electrochemical anodizing has a wide range of unique properties and is a promising material for creating various new-generation devices [1-7]. It is known that por-Si can have a wide range of porosity (from 2 to 90%) depending on the conditions of electrochemical treatment, the level of doping with donor or acceptor impurities, the composition of the electrolyte, etc. It is obvious that por-Si with a specific pore volume of several percent and por-Si with the highest porosity inevitably differ from each other not only in structural but also in optical, luminescent, and electrical properties. The use of por-Si layers as active elements in these devices requires careful study of the electrical properties of this material.

In [8], current-controlled switching was observed in the p-type crystalline silicon (p-c-Si) / porous Si (PS) / hydrogenated amorphous n-type silicon (n-a-Si: H) heterostructure. The most noticeable characteristic of a sharp increase in current at a voltage of ~ 0.95 V with a direct measurement from 0 to 1.8 V and a sharp decrease at 0.78 V with a reverse measurement was obtained, forming a loop. It is noteworthy that both forward and reverse switching occurs at the same current value of 10.8 mA. A switching mechanism is proposed that takes into account the presence of trapped carriers at the silicon-nanocrystal-SiO_x interface. This is because parts of the captured charges were bound near the n-a-Si: H / PS and PS / p-c-Si interfaces, forming an additional Coulomb barrier for the main carriers. It was assumed that when a voltage is applied to the PS layer, the captured carriers destroy the barrier at a certain threshold value and promote switching.

In memory devices, generators, and fast switching devices, one of the important electrical characteristics is the negative differential resistance (NDR) – a local increase in the current [9]. NDR is observed in devices made of amorphous silicon/silicon carbide [10], Si/SiO_2 nanowires, and devices based on quantum dots [11], as well as in porous silicon [12,13]. In [14], the NDR was investigated for a Schottky diode made of porous silicon. It is shown that thin filaments in porous silicon have much lower electron mobil-

ity than thick filaments due to electron scattering on the surface. Some carriers can overcome the gap in the conduction band and flow into thin filaments. The negative differential resistance was due to the difference in the mobility of thick and thin wires in porous silicon.

In [15], we studied the performance characteristics of memristive devices depending on the annealing temperature of thin films of zinc oxide (ZnO) over porous silicon (PSi) in a two-layer configuration. Electrical characteristics demonstrated that the psi nanostructured substrate and the configuration of ZnO layers effectively contribute to an 8-fold increase in the memristive ratio. The effect of a single-layer ZnO-PS configuration with single and different annealing resulted in continuous and sudden switching. The tests revealed a decrease in the switching coefficient with an increase in the voltage step size.

The volt-Farad characteristic (CV) of porous silicon at room temperature is given in [16]. Very clear quasi-periodic oscillatory features were found at voltage values in the range from -50 V to 50 V. This is because the low-dimensional quantum restriction in the PC is a possible reason for the observed CV fluctuations at room temperature.

CV characteristics of carbon nanotubes deposited on layers of porous silicon were studied in [17]. CV curves taken using a frequency of 1 MHz and an RMS value of 20 mV showed that the capacitance decreases with increasing voltage. This decrease was non-exponential and the capacitance became constant at high voltages. This behavior has been observed and attributed to an increase in the depletion region, that is, an increase in the built-in voltage. The sample etched for 4 minutes had a negative capacity of about 5 V. Negative capacitance is related to the non-monotonic or positive behavior of the transient current derivative in response to a small voltage jump.

Memristive devices are made of nanostructured composites of porous silicon-metal oxide (ZnO and VO_2) [18, 19]. Electrical characteristics indicate that both devices have symmetrical zero-crossing hysteresis curves typical of memristive systems. Although both devices showed significant durability and stable switching coefficient, the ZnO-based device showed relatively better stability and a higher resistive switching coefficient of 86% compared to the VO_2-based device.

From a brief review, it should be concluded that the volt-ampere and volt-farad characteristics of semiconductor nanofilaments and nanofilms, as a rule, have non-monotonic oscillating curves with the presence of hysteresis loops and sections of negative differential resistance. However, universal approaches to describing processes on this issue have not yet been established. Currently, there is no general theory explaining the features of nonlinear electrical conductivity of nanocluster semiconductor films depending on their nanoscale structure.

The purpose of this work is to experimentally study the volt-ampere and volt-farad characteristics of semiconductor nanoporous structures and search for characteristic general patterns.

2 Materials and methods of work

Measurements of the current-voltage characteristics of porous silicon films were carried out on the Ni EL VIS II+ educational platform (figure 1), with and without exposure to 630 nm infrared laser films in the voltage range from 0 V to 2 V. This platform is competitive measuring equipment in the field of circuitry, control systems, and telecommunications.

Samples of porous silicon with a p-n structure and dimensions of 8 x 2 mm^2 were obtained by electrochemical etching. The etching time of the films was 3 min, and the current density was 50 mA / cm^2. As the initial substrate, the prepared monocrystalline silicon with the p-n^+ junction was used, where n^+ – layer diffusion is a gradient of the impurity of phosphorus with a concentration of main charge carriers 10^{19} cm^{-3} with a gradual decrease of the impurity to the boundary of the p-n junction. The thickness of the p-silicon was 350 microns with a resistivity of 10 Ohm×cm, and the thickness of the n-layer was about 500 nm. To remove phosphor silicate glass, the silicon surface was etched in a 10% solution of hydrofluoric acid and washed in isopropyl alcohol using an ultrasonic device, and then dried.

To study the dependence of electric current on voltage, as well as capacitance on voltage, Inga contacts with a thickness of 370 nm each were applied to nanoporous films.

The volt-farad characteristics of nanostructured and porous silicon samples were measured using an Agilent E4980A LCR meter (figure 2) under natural light and laser exposure in the voltage range from 0 V to 2 V and from 2 V to 0 V. The Agilent E4980A Precision LCR-Meter (figure 2) operates in the frequency range from 20 Hz to 2 MHz. The basic accuracy of the equipment is 0.05 %. The device has excellent reproducibility of measurements at low and high impedance values.

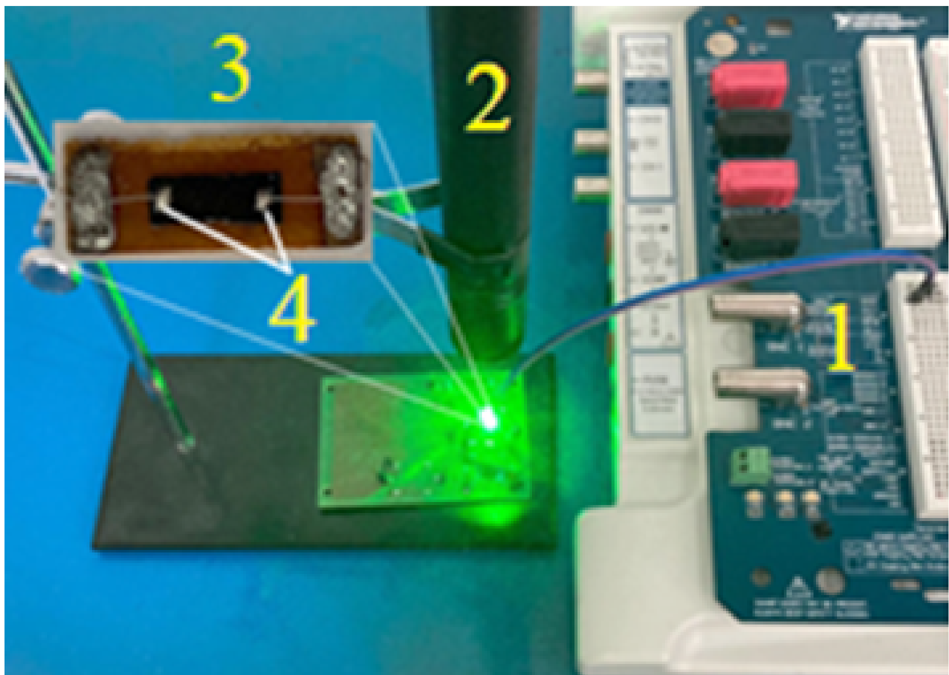

Figure 1 − Experimental setup: 1 – Ni EL VIS II + Platform,
2 − infrared laser, 3 – a porous silicon film, 4 − contact points on the film

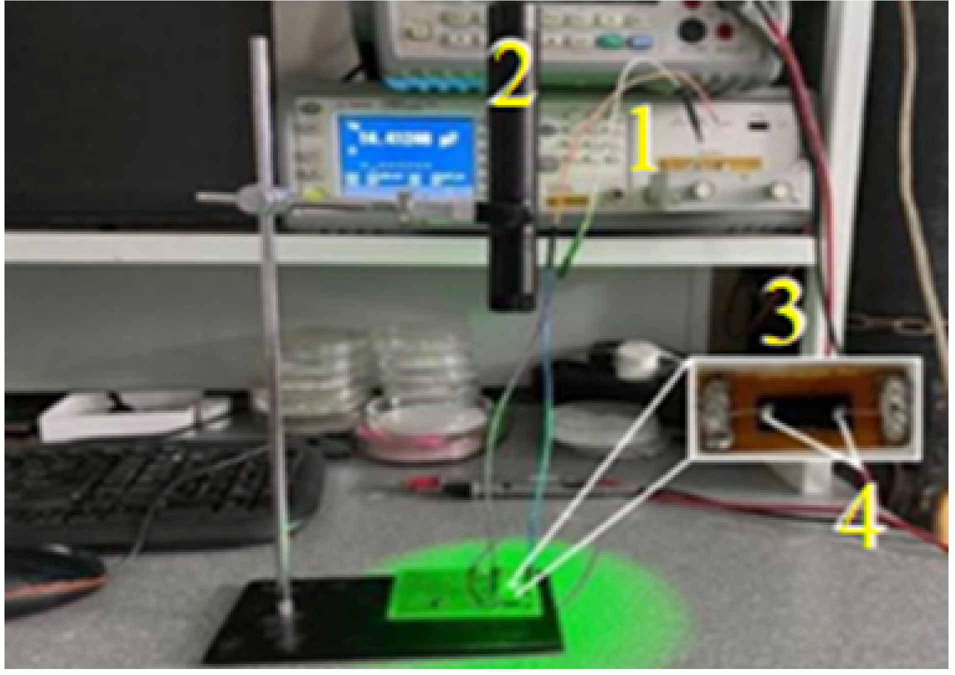

Figure 2 − Experimental setup: 1 − LCR meter the Agilent E4980A,
2 − infrared laser, 3 − a porous silicon film, 4 − metal contact

3 Experimental results and discussion

Figures 3 show the dependences of the electric current on the voltage of the VAC of porous silicon films with and without exposure to infrared laser radiation. In the range from -3 V to 3 V (figure 3(a)) – in natural light, from -2 V to 2 V (figure 3(b)) – when exposed to a laser, the VAC curves are characterized by the presence of oscillation, negative differential resistance, and hysteresis.

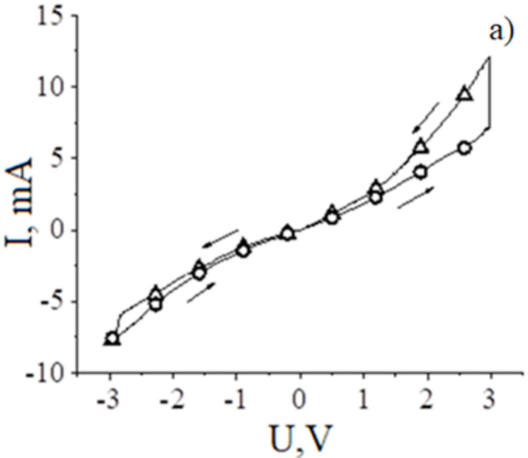

Figure 3 (a) − The volt-ampere characteristics of porous silicon in natural light.
Δ – for direct measurement,
○ − for reverse measurement

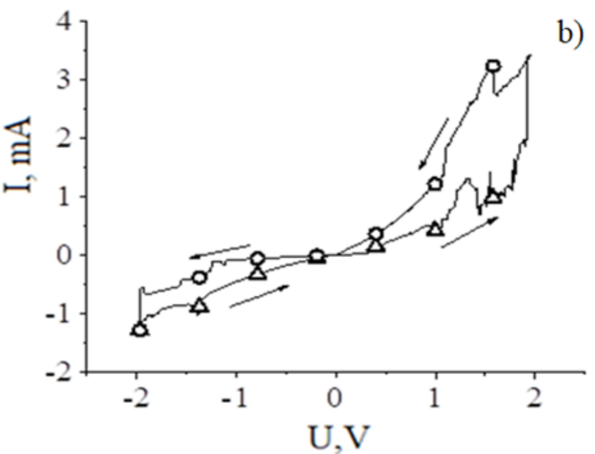

Figure 3 (b) − The volt-ampere characteristics of porous silicon when exposed to a laser.
Δ – for direct measurement,
○ – for reverse measurement

The nonlinear behavior of the VAC is typical, which can be explained by the dependence on the voltage of potential barriers in the structure of nanocrystal silicon. The experimental graph is characterized by the asymmetry of the hysteresis loops at forward and reverse (U<0) currents. The reverse current is significantly (~3 times) less than the forward current (U>0) under laser illumination. In this case, the current switching peaks are observed. Without laser action, current surges are not observed.

The difference in the shape of the curves during repeated transmission of current through the film indicates a change in its structure and the presence of memristive properties of the film.

Figure 4 shows the volt-farad characteristics of a porous silicon sample obtained at different frequencies (f) of the external voltage U (f) under the influence of a laser and in natural light.

The volt-farad characteristics in the form of hysteresis are obtained when the voltage increases from 0 V to 2 V, and then when it decreases. In natural light, the capacitance value decreases and stabilizes as the voltage increases. In natural light, a sample of porous silicon has properties similar to the metal-dielectric-semiconductor structure [22]. When a laser beam is applied to a porous silicon sample, the electrical capacity at a constant charge is inversely proportional to the voltage. The energy of the laser beam increases the energy of additional charge carriers in the valence band to the level of the conduction band, which increases the capacitance value. In figure 4 (a), when illuminated by a laser beam, a negative capacitance value is observed, with a low voltage value. As noted in [20], negative capacitance occurs due to a monotonous transient process with a small change in voltage, i.e., due to a decrease in charge.

Figure 5 shows the volt-farad characteristics of a porous silicon sample in natural light, under laser and incandescent illumination at a voltage frequency of 100 kHz.

Table 1 shows the areas of the hysteresis curves of the volt-farad characteristics obtained under different lighting conditions in conventional units. The area of the hysteresis curves obtained by laser and lamp illumination of the film increases by 2.54 and 1.87 times. When simultaneously illuminated with a laser and a lamp, an increase in the area of 4.5 times is observed.

Figure 4 − The volt-farad characteristics of a porous silicon sample, frequency f (kHz):
(a) − 1, (b) −10, (c) − 10^2; (d) −10^3
Δ − in natural light conditions; ○ − when illuminated by a laser beam

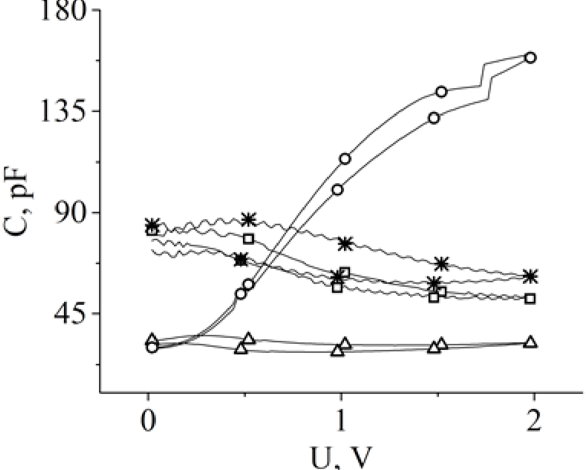

Figure 5 − The volt-farad characteristics
of porous silicon samples: Δ – in natural light,
○ − under laser illumination, □ – under illumination

Table 1 – Changes in the hysteresis characteristics under different illumination of the nanofilm. S_0 is a value of S in natural light

Type of lighting	Conditional hysteresis area (S)	S_x/S_0
Natural	5.23	-
Laser	13.33	2.54
Lamp	9.78	1.87
Laser+lamp	23.55	4.5

Figure 6 shows the change in the volt-farad characteristic when a voltage is applied from 0 V to 2 V, at a voltage frequency that coincides with the characteristic size of the nanofilm (~10^{-3}m) and the propagation speed of the electromagnetic wave (~10^8m/s). The resonant decrease in the capacitance (~10^5Hz) is observed.

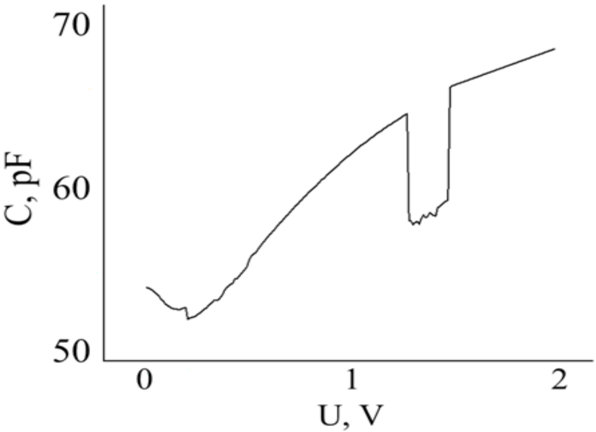

Figure 6 − The volt-farad characteristic of a porous silicon sample at 100 kHz

There is an abrupt decrease in the capacitance in the voltage range 1.2-1.4 V, comparable to the value of the width of the energy-forbidden zone of silicon. A sharp decrease in the capacitance value is associated with a decrease in the charge when the voltage is resonant.

Figure 7 shows the dependence of capacitance on the frequency at a constant voltage value.

As the frequency increases, the capacitance value decreases. This means that porous silicon structures have depletion and charge accumulation zones, as in metal-dielectric-semiconductor devices.

At low frequencies, the capacitance value is higher, since the conditions of the boundary loop are in equilibrium. At high frequencies, the capacitance is related to the spatial distribution of charges, and the boundary conditions of the loops are not affected by the voltage [22]. A similar result was obtained in [19, 21, 22].

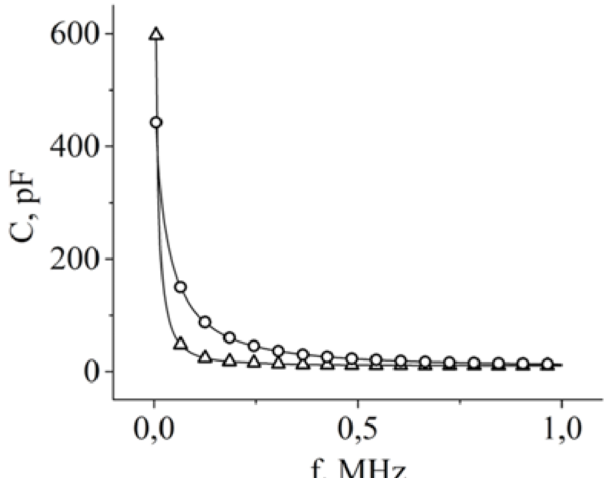

Figure 7 – The frequency dependence of the capacitance at a constant voltage U = 1 V, Δ − in natural light; ○ − in laser light

4. Conclusion

The various qualitative and quantitative changes in the electrical conductivity and electrical capacity of nanoporous semiconductor films are shown experimentally. Some general regularities are established: non-linear, hysteresis dependence of electric current, electric capacity on voltage both in natural light and under laser radiation. In the latter case, the characteristics increase up to 3-4 times. The appearance of chaotic bursts jumps in changes in electric current and capacitance is observed at external voltage values close to the value of the energy band gap of the semiconductor. As the process repeats, the structure of the nanofilm changes: the conductivity increases, and the resistance decreases. These phenomena of current switching and memristor behavior of the capacitance can also be realized on spatial scales of the order of a micron, as resonant effects of the characteristic frequencies of the film and external perturbation.

The established experimental facts can serve as a basis for improving the nanotechnology of memory elements, sensors, photo converters, and for building the necessary physical theories.

References

1. Praveenkumar S., Lingaraja D., Mathi P.M., Ram G.D. An experimental study of optoelectronic properties of porous silicon for solar cell application // Optik. -2018. –Vol. 178. –P. 216-223.

2. Bisi O., Ossicini S., Pavesi L. Porous silicon: a quantum sponge structure for silicon based optoelectronics // Surface Science Reports. -2000. –Vol. 38. –P. 1–126.

3. Skelton J.M., Pallipurath A.R., Lee T.-H., Elliott S.R. Atomistic origin of the enhanced crystallization speed and n-type conductivity in Bi-doped Ge-Sb-Te phase-change materials // Advanced Functional Materials. -2014. –Vol. 24. –No. 46. –P. 7291-7300.

4. Wang B., Qiu J., Feng H., Sakai E., Komiyama T. KOH-activated nitrogen doped porous carbon nanowires with superior performance in supercapacitors // Electrochimica Acta. -2016. –Vol. 190. –P. 229–239.

5. Ibraimov M.K., Sagidolda Y., Rumyantsev S.L., Zhanabaev Z.Zh., Shur M.S. Selective gas sensor using porous silicon // Sensor letters. -2016. –Vol.14. –No.6. –P. 588-591.

6. Bennett M.F., Bittner Z.S., Forbes D.V., Tatavarti S.R., Ahrenkiel S. P., Wibowo A., Pan N., Chern K., Hubbard S.M. Epitaxial lift-off of quantum dot enhanced GaAs single junction solar cells // Appl. Phys. Lett. -2013. –Vol. 103. –No.21. –P. 213902.

7. Ge D., Shi J., Wei J., Zhang L., Zhang Z. Optical sensing analysis of bilayer porous silicon nanostructure // Journal of Physics and Chemistry of Solids. -2019. –Vol. 130. –P. 217-221.

8. Chakrabarty S., Mandal S., Ghanta U., Das J., Hossain S.M. Current controlled switching in Si/PS/a-Si heterostructure // Materials Today: Proceedings. – 2018. – Vol. 5. – No. 3. – P. 9790-9797.

9. Nam Do V., Dollfus P. Negative differential resistance in zigzag-edge graphene nanoribbon junctions // Journal of Applied Physics. -2010. –Vol. 107. –No. 6. –P. 063705.

10. Chen K.H., Fang Y.K., Shieh K.H., Liou W.R. Preparation and analysis of the negative resistance characteristic in an amorphous silicon and silicon–carbide single-barrier device // Applied physics letters. -1994. –Vol. 65. –No. 22. –P. 2815-2817.

11. Yu L.W., Chen K.J., Song J., Wang J.M., Xu J., Li W., Huang X.F. Coulomb blockade induced negative differential resistance effect in a self-assembly Si quantum dots array at room temperature // Thin Solid Films. -2007. –Vol. 515. –No. 13, -P. 5466-5470.

12. Lee M.K., Chu C.H., Tseng Y.C., Shyr J.M., Kao C.H. Negative differential resistance of porous silicon // IEEE Electron Device Letters. -2000. –Vol. 21. –No. 12. –P. 587-589.

13. Marin O. et al. Negative differential resistance in porous silicon devices at room temperature // Superlattices and Microstructures. -2015. –Vol. 79. –P. 45-53.

14. Martínez L., Becerra D., Agarwal V. Dual layer ZnO configuration over nanostructured porous silicon substrate for enhanced memristive switching // Superlattices and Microstructures. -2016. –Vol. 100. –P. 89-96.

15. Lee M. K. et al. Negative differential resistance of porous silicon // IEEE Electron Device Letters. -2000. –Vol. 21. –No. 12. –P. 587-589.

16. Betty C. A. Highly sensitive capacitive immunosensor based on porous silicon–polyaniline structure: Bias dependence on specificity // Biosensors and Bioelectronics. -2009. –Vol. 25. –No. 2. -P. 338-343.

17. Mkhitaryan Z. H. et al. I–V characteristics of structures with porous silicon in electrolyte // Optical Materials. -2005. –Vol. 27. –No.5. –P. 962-966.

18. Ocampo O., Antúnez E. E., Agarwal V. Memristive devices from porous silicon–ZnO/VO_2 nanocomposites // Superlattices and Microstructures. -2015. –Vol. 88. –P. 198-203.

19. Garzon-Roman A., Milosevic O., Rabanal M. E. Morphological, structural, and functional properties of vertically aligned carbon nanotubes deposited on porous silicon layers by ultrasonic spray pyrolysis // Microporous and Mesoporous Materials. -2020. –Vol. 292. –P. 109738.

20. Sancho A., Arizti F., Gracia F. J. Porous silicon for the development of capacitive microstructures // Microelectronic engineering. -2009. –Vol. 86. –No.11. –P. 2144-2148.

21. Kaur R., Arora A., Tripathi S. K. Fabrication and characterization of metal insulator semiconductor Ag/PVA/GO/PVA/n-Si/Ag device // Microelectronic Engineering. -2020. –Vol. 233. –P. 111419.

22. Gabouze N., Belhousse S., Cheraga H., Ghellai N., Ouadah Y., Belkacem Y., Keffous A. CO_2 and H_2 detection with a CH_x/porous silicon-based sensor // Vacuum. -2006. –Vol. 80(9). –P. 986-989.